Report on developed research techniques using microscopy and associated sciences in an international setting

By

Mitchell Dyen

A paper submitted in fullfillment of the requirements
for IRES NSF Project #1952513

Okazaki, Japan
2024

PI: Yasuhiro Kamei

Abstract:
During the summer of 2024 I visited Dr. Yasuhiro Kamei's lab at the National Institute for Basic Biology in Okazaki, Aichi, Japan. His lab has many interdisciplinary projects focused on developing new microscopy methods such as IR-LEGO, material design, and establishing transgenic lines all using *Oryzias latipes*, also known as medaka fish, as a model organism. There are many techniques involved in the Kamei lab that I was unfamiliar with, so this summer my goal was to be exposed to as many different new techniques as possible that I am not exposed to at my home lab. These techniques include operating confocal microscopes, spinning disk microscopes, scanning electron microscopes, atomic force microscopes, light sheet microscopes, plasmid design, plasmid purification, bacteria transformation, cell culture, glass silanization, cre/loxp, and finally IR-LEGO. Being exposed to these methods has given me new tools to broaden my research ventures, and has given me reasons to reach out to other scientists at my home university of University of Central Florida for collaboration opportunities in using their equipment. Most of the projects I worked on are still in progress and as such I cannot make conclusions, so this paper will be a review of the techniques I have learned over the course of my stay in Japan.

Introduction: **IR-LEGO**
Temperature is an important parameter for living organisms. There are vast amounts of body systems dedicated to regulating body temperature, along with many different environmental temperatures that organisms function in. Given so much variance on a large organism level, this leads to Kamei's research regarding temperature analysis on a cellular/molecular level. This field has been coined biothermology and is characterized by investigating the nature of temperatures in living organisms ranging from nano to micro. The techniques involved with biothermology that I was exposed to involved IR-LEGO. IR-LEGO: InfredRed Laser Evoked Gene Operator (Kamei et al, Nat. Methods 2009) is a local heating technique used in combination with fluorescent proteins known as gTEMP (Nakano et al, PLoS One 2017).

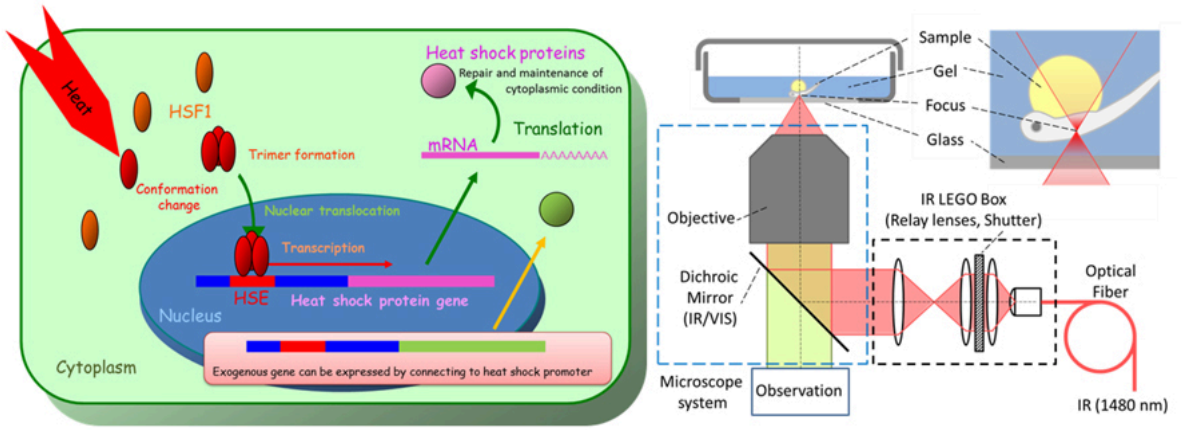

Figure 1. IR-LEGO structure and gene expression induction

The left side is displaying how heatshock factor 1 (HSF1) activates transcription inside of a cell. The right side shows the structure of the IR-LEGO machine (Kamei et al, Nat. Methods 2009)

These fluorescent proteins can rapidly respond to a wide temperature range and then be observed with various microscope systems. gTEMP can be expressed invivo through transgenic lines. The lines we used were gaudi lines, expressing multiple different fluorescent proteins. If Medaka are exposed to IR-LEGO alone, the heat shock response is transient and not traceable after a period of time. In order to create a permanent expression change, Cre/Loxp recombination system is used. Irradiated cells are permanently labeled and lineage is able to be tracked by fluorescent proteins. It was extensively used as a tool for cell-fate mapping in (Shimada et al, Nat Commun. 2013).

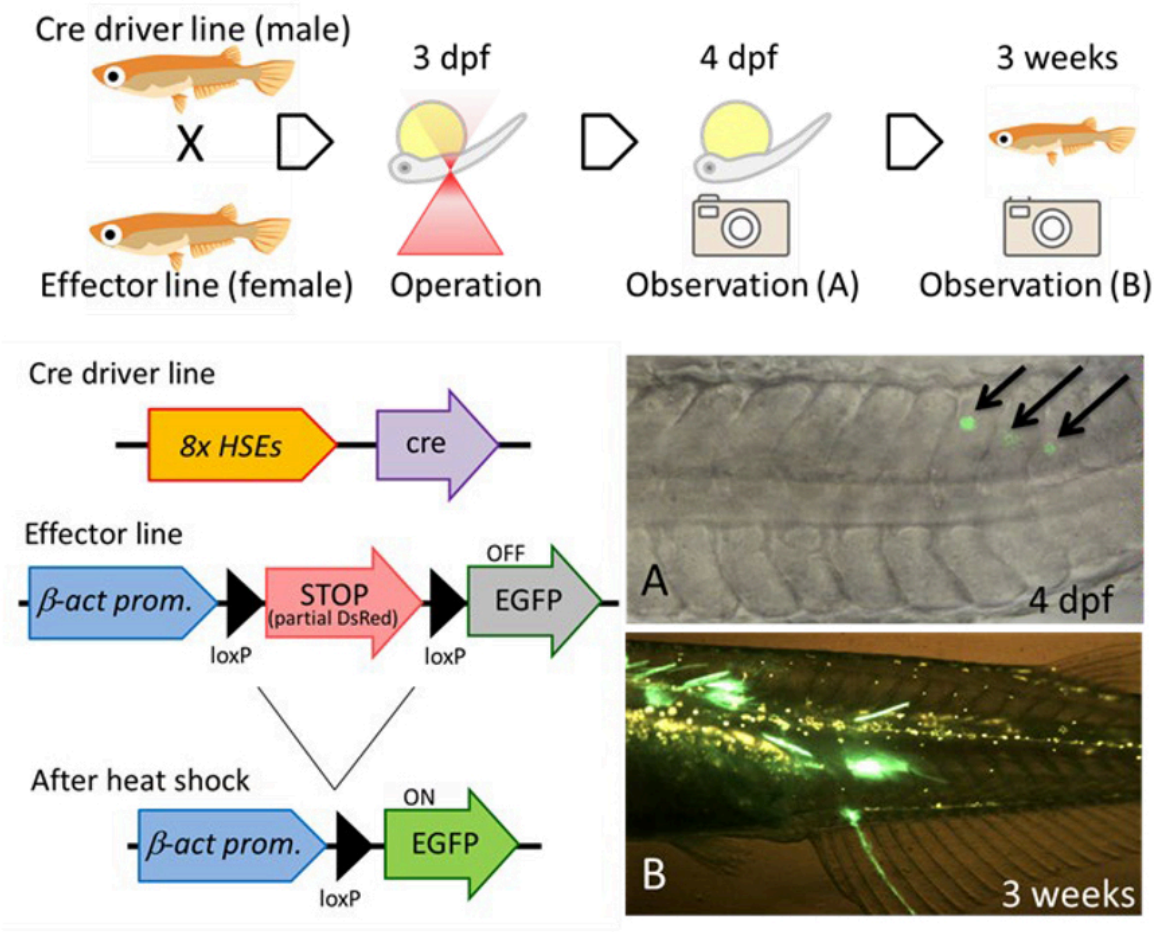

Figure 2. Long-term gene expression system with cre/loxp recombination system (Shimada et al, Nat Commun. 2013)

Light sheet microscopy is used for creating high quality 3D models of clear samples. It does this by taking many small thin slice images of the sample and compiling them into one 3d model. You can adjust how many slices you would like, but the machine is very fast at taking images and can produce high quality models in a minimal amount of time. I used confocal along with light sheet microscopy to analyze the effects of IR-Lego on a

juvenile gaudi madaka. Refer to microscopy section for more information

Methodology for IR:LEGO experiment

We applied a short 1, 1.5 and 2 second blast from the infrared laser across three medaka. They were anesthetized with MS.222. Three blasts were applied, evenly spaced a few milimeters, on the skin of the medaka five vertibrates from the tail fin, and the next three were targeted at the inner muscle mirrored to the previous three blasts on the opposite side of the vertibrate. The wattage of the laser was changed for each fish. 18mW, 20mW. 22.5 mW. We then observed fluorescent protein expression using confocal and light sheet microscopy.

Our positive control fish was put in a hot water bath and experienced whole body heatshock. Our negative control was only exposed to room temperature conditions

Results

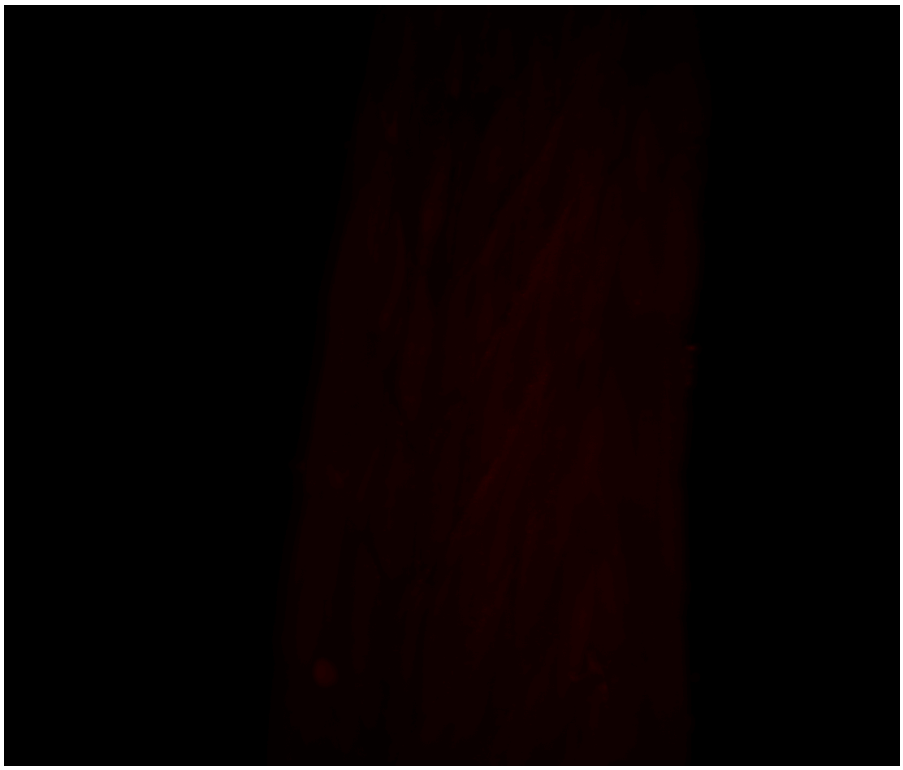

Figure 3. lightsheet image of negative control medaka expressing RFP lightsheet

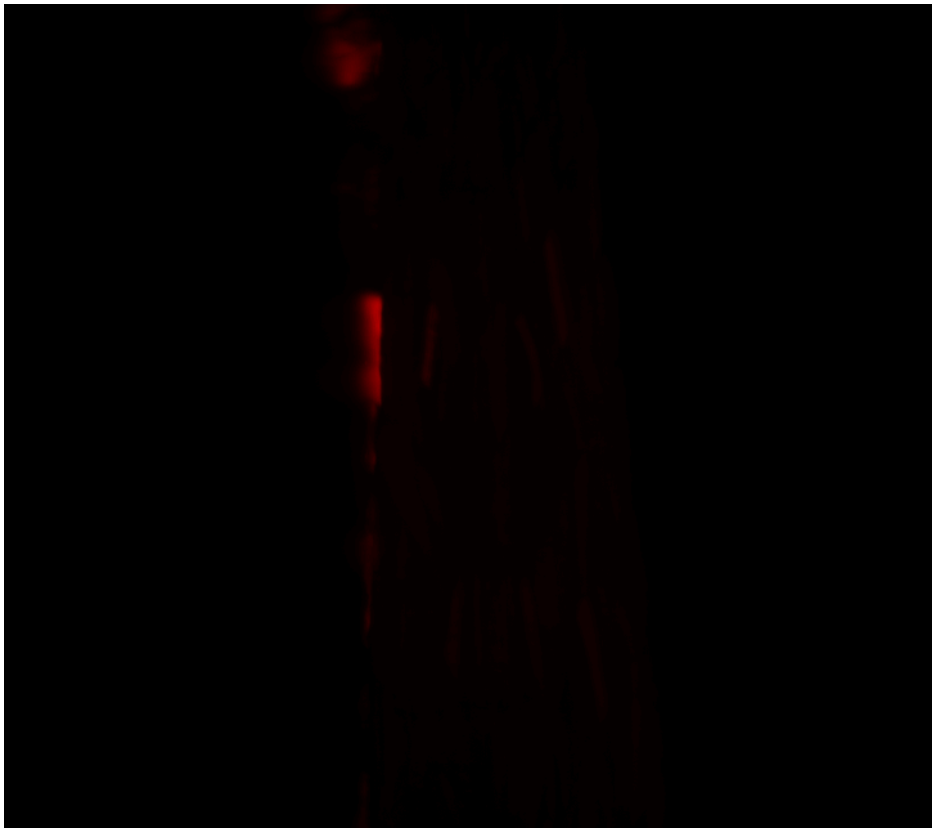

Figure 4. lightsheet image of positive control medaka also expressing RFP lightsheet

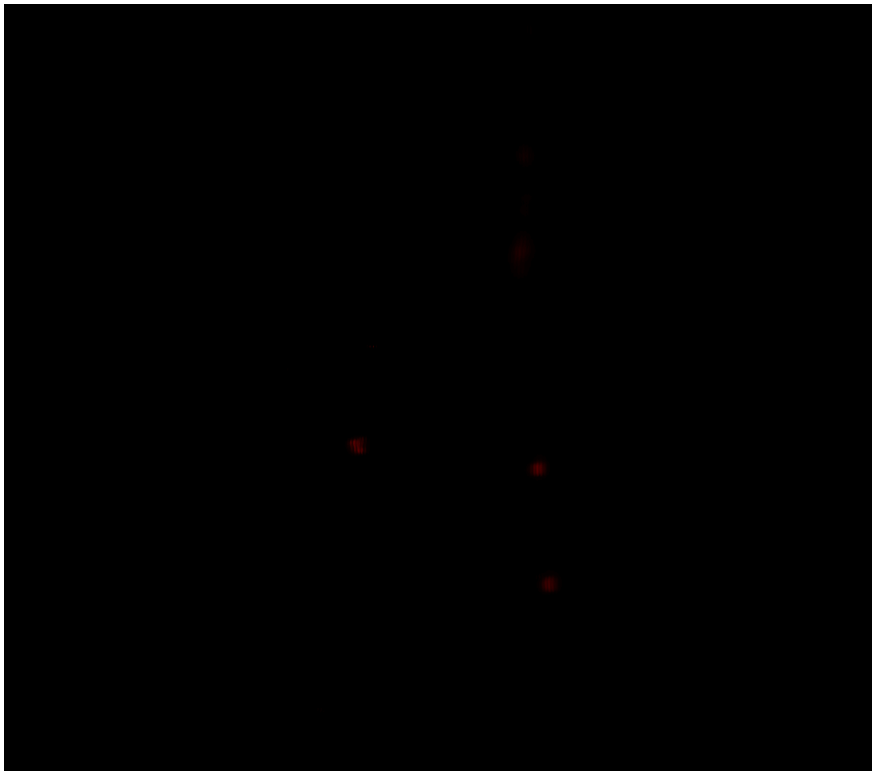

Figure 5. lightsheet image of 20 mW IR-LEGO exposed fish showing points of exposure

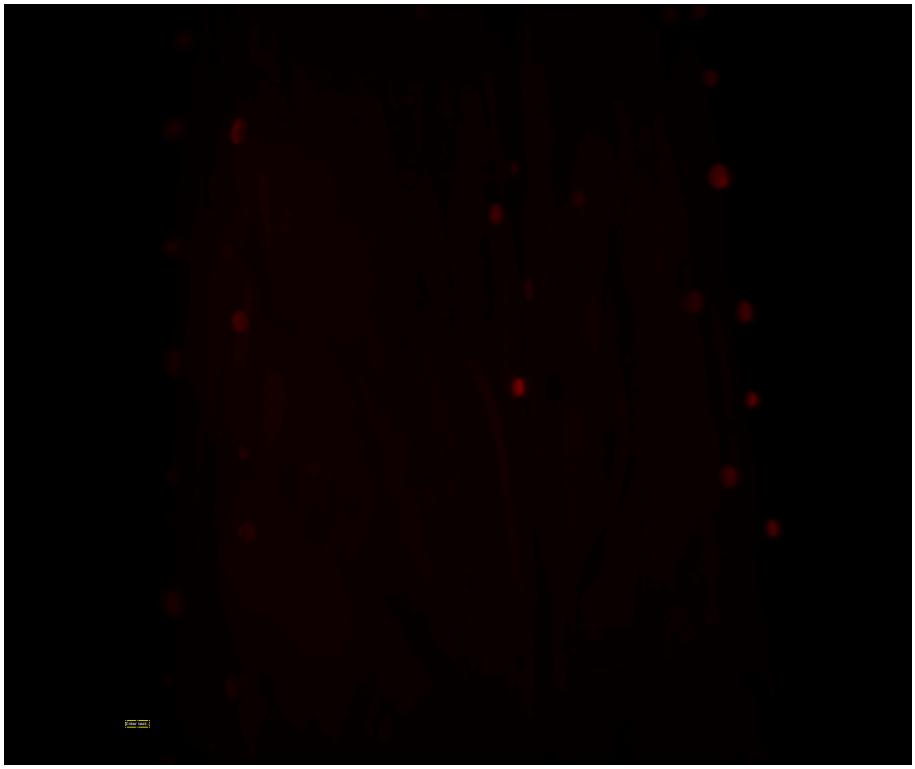

Figure 6. 1 lightsheet image of 8 mW IR-LEGO exposed fish showing points of exposure, but also natural flourescence

Discussion

Our results are hard to make conclusions on for multiple reasons.

The first issue was with our wattage selection. Originally we started at 20 mW and were climbing to 22.5 mW and 25mW, but at 22.5 mW we observed blasting a hole in the fish with the IR-Lego laser. This is obviously not a desired effect so we instead decided to lower the voltage and test 18mW.

Our second issue was we were unable to detect fluorescence caused by the IR-Lego using a basic laser microscope. It could only see the natural fluorescence of fish. We tested multiple wavelengths of laser, as the fish we were targeting was a Gaudi line meaning it expresses multiple fluorescent proteins, but we were unable to distinguish between our target site and the fish's normal amount of fluorescence. Our conclusion moving forwards was to use the Leica Sp8 as it is a much more sophisticated microscope and has more available wavelengths because it has more lasers attached.

The Leica SP8 had similar issues to the basic laser microscope, but some samples we thought that it could possibly be detecting the IR-Lego site. It was still unclear in the samples so we elected to take it even further by using a light sheet microscope.

Even with the light sheet microscope, we had strange occurrences such as our positive control very faintly expressing RFP (red fluorescent protein). Another occurrence is our negative control expressing this RFP while it should not be doing so, even brighter than our positive control. The transgenic line that these fish belong to should only be expressing RFP when undergoing heatshock.. Furthermore, our target points along the fish's tail have naturally occurring fluorescent protein points that are very difficult to discern from our IR-LEGO blasts. We think there may have been a mistake in the original sourcing of transgenic fish from the tank, or a silencing mutation occurred. I also accidentally squished one of our fish representing 22.5 mW so that data point is no longer available.

Introduction: **Glass Silanization**

Glass silanization attaches an organosilyl group to a glass surface, causing it to become non-polar. Its non-polar nature will cause the surface to be hydrophilic. The reasoning behind wanting to silanize glass is to provide a clear-hydrophobic surface to spread water evenly across its surface, vs a normal hydrophilic surface that leads to beads of water. This also leads to the gel being chemically bonded to the glass and not having any imperfections (Figure 3). Combining a hydrophilic surface with a hydrophobic surface in a sandwich fashion lets us get an extremely thin layer of gel that is ideal for AFM testing.

We used this to observe the differences in shape and spread of muscle stem cells based on rigidity of the gel surface.

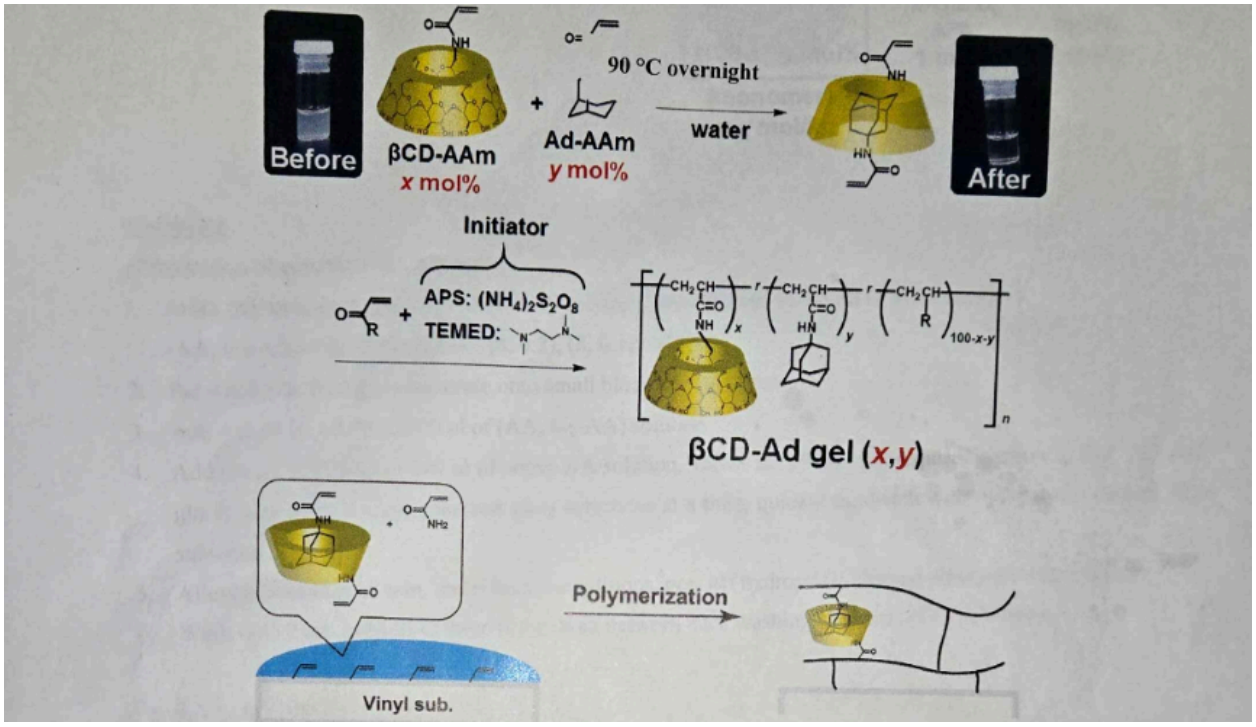

Figure 7. Visualization of molecules at the surface of silanized glass bonding to gel (191118 Masaki Nakahata & Kentaro Hayashi)

Methodology

Cleaning:

Immerse glass slides in following solvent and apply ultra-sonication with sonication bath

1. Acetone (3 minutes, room temperature)
2. Ethanol (3 minutes, room temperature)
3. Methanol (3 minutes, room temperature)
4. MilliQ Water (3 minutes, room temperature)

In chemical hood, immerse glass slides into acid-base mixture H2O2:NH4OH:MilliQ = 1:1:5

1. Ultra-Sonicate (3 minutes, room temperature)
2. Hot water bath (45 minutes, 60C)

Rinse 10 times with MilliQ to remove residual solution

Dry glass slides in vacuum drying oven (70C)

We set aside half of the slides on this step as they are hydrophobic, needed for the sandwich. The other half were sialanized.

Silanization:

1.Set hydrophobic glass substrates onto substrate holder, put in reaction tank

2.Add vinyltrimethoxysilane solution, 190mL Toluene, 10mL Vinyltrimethoxysilane, and shake overnight room temperature
3.Remove vinyltrimethoxysilane solution, add toluene, ultrasonic (3 minutes, room temperature)
4.Remove toluene, add ethanol. (3 minutes, room temperature)
5.Remove ethanol, add MilliQ. (3 minutes, room temperature)
6. Rinse 10 times with MilliQ
7. Dry in vacuum oven overnight (70C)

A bis-acrylamide gel solution is then created and applied to the gel

1.Make AA, bis-AA solution by mixing 1 mL of solutions
(AA, bis-AA) = (8, 0.8) , (8, 0.4), (8, 0.2), (8, 0.1) (w/v%)
2. Put vinyl-silanized glass substrate onto a small block on wet paper
3. Add 4 uL of 50x APS to 200uFL of (AA, bis-AA) solution
4. Add 0.9 uL of TEMD to 200 uL of AA solution, cortex 10 sec, put 45 uL onto vinyl–silanized glass substrate, quickly sandwich hydrophilic cleaned glass substrate
5.Allow to stand for 15 minutes under humid conditions, peel of hydrophilic cleaned glass substrate with care
6. Wash with 2mL of Milli-Q three times, Wait between each washing step at least 1h x3 times

An atomic force microscope was used to make sure the kPa of the gel was relatively in the ballpark of muscle stem cell conditions (8-12 kPa).

Muscle stem cells were then applied to the surface of the gel and incubated overnight

The cells were then observed under a phase contrast microscope and snapshots of the plate were taken

The snapshots were then observed in Fiji, a image processing package, where cells were circled. Fiji calculated their area and aspect ratio and then those results were averaged and created into a chart.

Results

Sample Name	Average Area	Area STDEV	Average AR	AR STDEV	Column1
KH 0.05	348.296575	183.2568949	2.77905	1.282389292	1.8
KH 0.1	375.981925	203.5375388	3.9983	2.358925276	6.6
KH 0.2	504.4502	225.1094672	3.422575	2.634468997	12
Glass Control	749.7373455	410.4495546	3.439072727	1.899643238	>GPa
0.05	442.9473091	197.406386	4.2342	2.412198412	1.8
0.2	555.2780167	278.7054015	4.4174	2.935657009	6.6

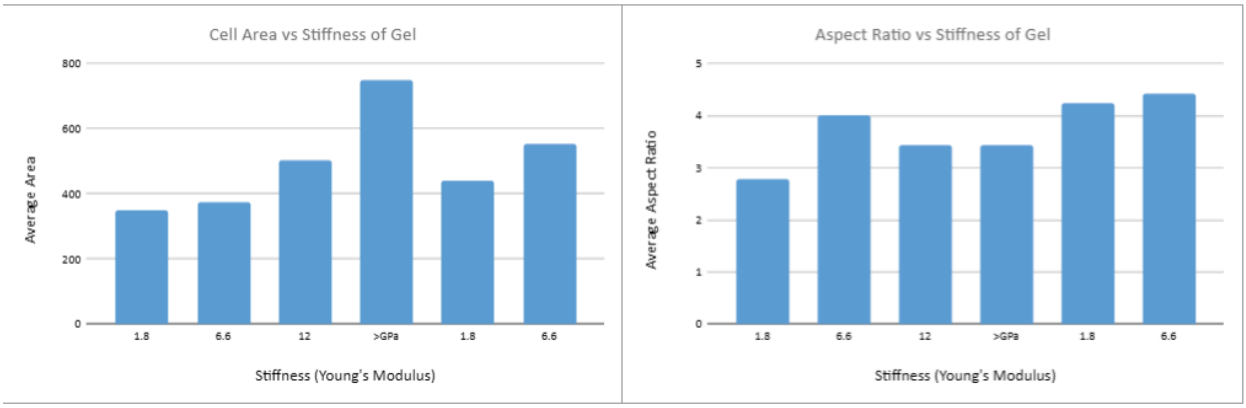

Figure 8. Silanized glass data

Discussion

Our findings were that the more stiff the surface, the larger the cell area. We also found that the shape of the cells was rounder the less stiff the substrate, as seen by the aspect ratio calculations. This could be due to a multitude of factors, one of them being small crevasses that formed in some of the softer substrates. This could cause the cells to sink into the creavasses and spread less and become more circular in shape. This data could be important in future experiments trying to emulate actual cellular size and spread, as the formulation AA-bisAAA ratio can effect those factors heavily.

Introduction: **Plasmid Design & Cell Culture**

Plasmids are small circular pieces of DNA found in bacterial cells. They are very unique as bacteria often transfer plasmids between themselves through horizontal gene transfer, making them very situated for introducing new genetic code into a baceria (Gull 2019). Multiple DNA elements can be introduced into plasmids through enzymatic cleavage and ligation, such as transcription factor binding sites and resistance genes, that makes them extremely useful for insertion into other organisms. Plasmids are manipulated primarily through purchasing a backbone plasmid from a biotechnology company, and then following their notations on recommended enzymes for certain cleavages at different points along the plasmid, and then you can add elements of your choosing to the backbone based on your desired location within the backbone as long as it is compatible with the element you want to introduce (Gull 2019). There are many

softwares to view these sites, but we used ApE. This summer I helped design a plasmid to be inserted into medaka eggs with the goal of binding mouse HSP70 (heat shock) promotor upstream of a mCherry/mNeonGreen fluorescent protein gene, along with a hygromycin resistance gene. Having a hygromycin resistance gene included in the desired plasmid allows us to introduce hygromicin into our LB agar plates, leaving only correctly transformed bacterial colonies being able to grow on the plate. The resulting transgenic line, when exposed to heat shock, would produce mCherry/mNeonGreen while being resistant to the hygromycin antibiotic.

As this was early in my summer experience, a lot of this was very new to me and moved very quickly with a large language barrier. Furthermore, when I was introduced to this project it was already in progress. Thus I am missing some information regarding the procedure list for the initial steps of enzymatic cleavage for our plasmid. This was a part of being in such a scientifically diverse lab, I was often ping-ponged to different projects rapidly.

Methodology

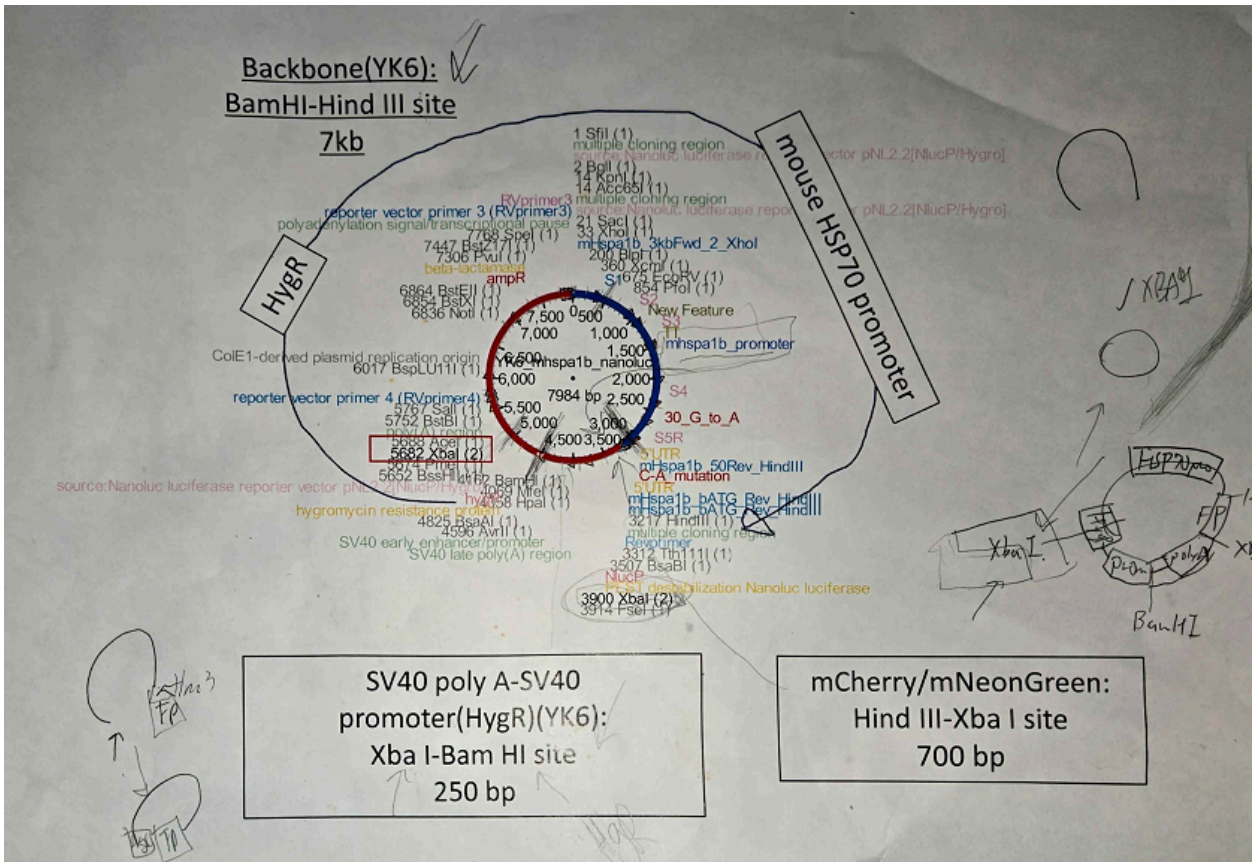

Figure 9. ApE plasmid design schema

We followed this scheme in order to make our desired plasmid. We started with a YK6

plasmid backbone, and made various enzymatic cuts in order to obtain the fragments we needed. We used XbaI-Bam HI to cut our HygR promotor, and HIND III- XbaI in order to source our fluorescent protein gene. After the cuts we recovered the fragments with electrophoresis and followed the FastGene Gel/PCR Extraction kit for the recovery of those fragments. We then recombined the desired fragments with our cleaved backbone and checked through electrophoresis to see if we had the desired complete plasmid. The backbone already contained a HSP along with the HygR gene, we only needed to add a fluorescent protein gene downstream from the HSP and a HygR gene promotor. Once we had our desired plasmid, we continued according to the procedure below.

1.) Thaw cells for five minutes
2.) Add 20 ng of purified plasmid DNA to cells in tube and mix by inversion
3.) Incubate cells on ice for 30 minutes
4.) Transfer cells to tube warmer set to 37 C for 45 seconds
5.) Transfer cells to ice for 2 minutes
6.) Incubate cells at 37C for 1 hour
7.) Pipette 20 uL of cell suspension onto LB hygromycin agar plates and spread using a sterile spreader
8.) Incubate plates over night in incubator set to 37C
9.)Select colony(s) from culture
10.) Culture the clone
11.) Digest plasmid using restriction enzyme ()
12.) Separate by gel electrophoresis
13.) Cut out desired band using scalpel

FastGene Gel/PCR Extraciton Kit
1.) Transfer up to 300 mg of gel slice into a microcentrifuge tube
2.) Add 500 uL of Binding Buffer GP1 to the sample and vortex
3.) Incubate at 55C for 10-15 minutes until gel slice is completely dissolved. Invert tube every 3 minutes
4.) Place a Column into a Collection Tube
5.) Transfer up to 800uL of the sample mixture from previous steps into the Column and centrifuge at 13,000 rpm for 30 seconds
6.) Discard flow-through and place Column back to Collection Tube
7.) Add 600uL Wash Buffer GP2 to the Column and centrifuge at 13,000 rpm for 30 seconds
8.) Discard flow-through and place the Column into a new Collection Tube
9.) Centrifuge again for 2 minutes at 13,000 RPM
10.) Transfer Column into a new microcentrifuge tube

11.) Add 25 uL of Elution Buffer GP3 to the center of the column matrix
12.) Allow to incubate for 2 minutes
13.) Centrifuge at 13,000 rpm for 2 minutes to elute purified DNA

Discussion

Learning about plasmid design and cell culture at the same time is very difficult, and we definitely had roadblocks along the way. Our initial batch did resist hygromycin, but did not have any bands that were suggesting the length we suggested. Essentially it seemed like our plasmids were uncut despite treating them with enzymes. We treated the plasmid with two enzymes and their desired lyse points were extremely close together, I think about 6base pairs. The plasmid instructions supplied by the manufacturer stated that despite their proximity, the two enzymes are perfectly suitable, but this was not the case in our experiment. This caused us to go back to the drawing board and inspect the plasmid with the ApE software and choose new enzymes. We repeated the process using new enzymes and it seemingly went fine, but also I started working on the sialanzied glass experiment and a Post-Doc took over the plasmid design fully, so I did not see the final results of the experiment.

Microscopy Techniques:

Light Sheet fluorescence microscopy uses a thin sheet of light to excite flurophores within the focal volume (Stelzer et al 2021). This means that light sheet microscopy can be used for highly detailed images of cleared samples in three dimensions by rotating the sample within the machine, along with two dimensions if desired. There is minimal background and out of focus light when comparfed to confocal or widefield microscopes. You can adjust how thin your light sheets are along with how many to take images of. The thinner the light sheet and more images you take will create a higher resolution image. There are many applications for vertebrate and invertebrate embryos, brains, cells, tissues and plants. In our scenario we used it on juvenile medaka which are conveniently already clear, so we did not need to include any clearing reagents.

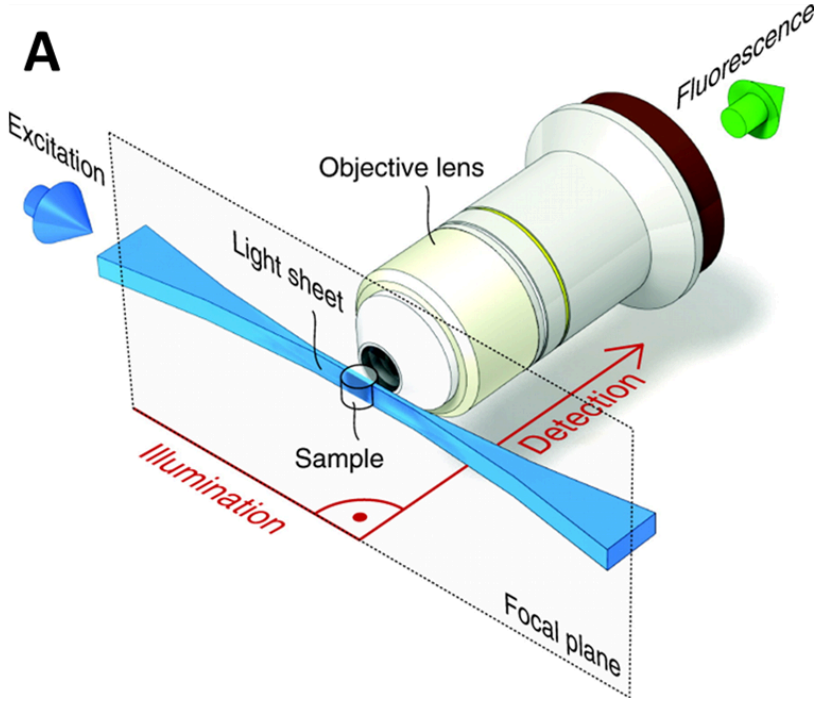

Figure 10. A light sheet microscopy imaging setup. (B. -C Chen 2014)

Confocal

Confocal microscopy is used to generate high resolution images of materials stained with fluorescent probes(Elliot AD 2020) In our case our fluorescent probes were fluorescent proteins such as GFP or TDTomato. This was the primary tool used in the Kamei lab for quick imaging of a fluorescent sample. It works by projecting a laser onto the sample through an objective lens. Multiple different confocal microscopes were used because they often had different lasers with different wavelengths equipped, which correspond to different fluorescent proteins. The construction schema can be seen below

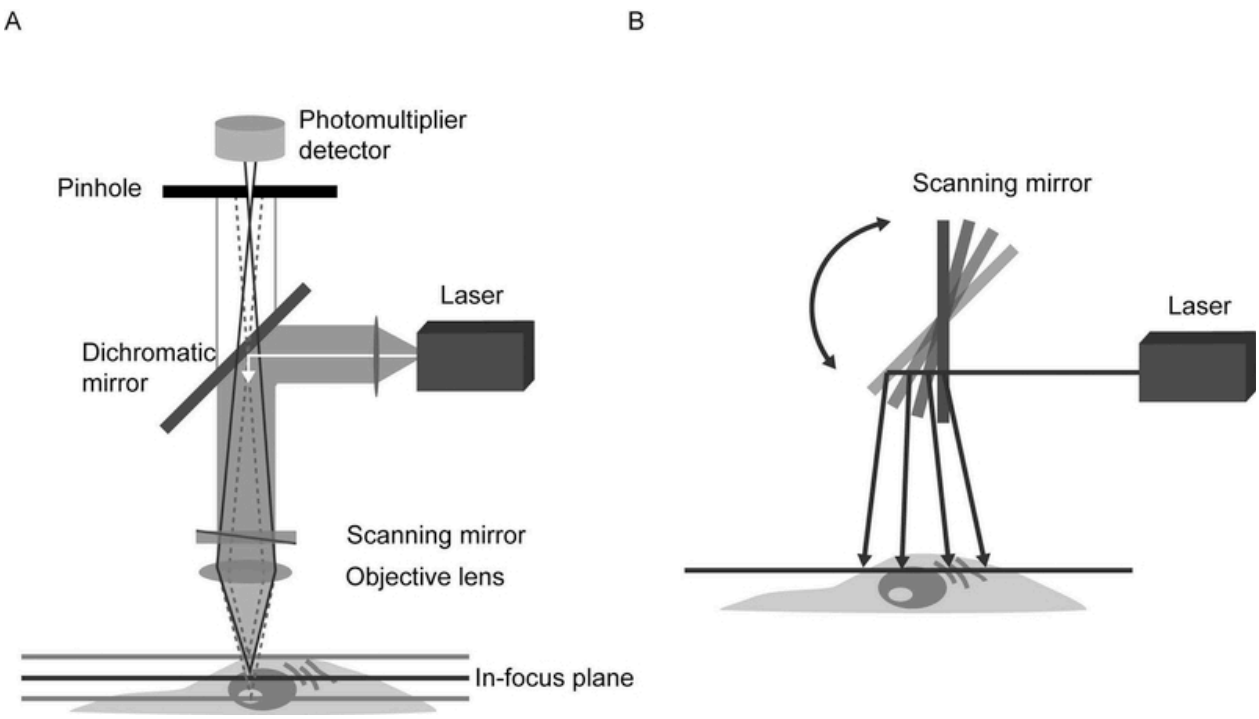

Figure 11. A. Construction of a confocal microscope B. Function of a scanning mirror sweeting excitation wavelength across sample (Elliot 2020)

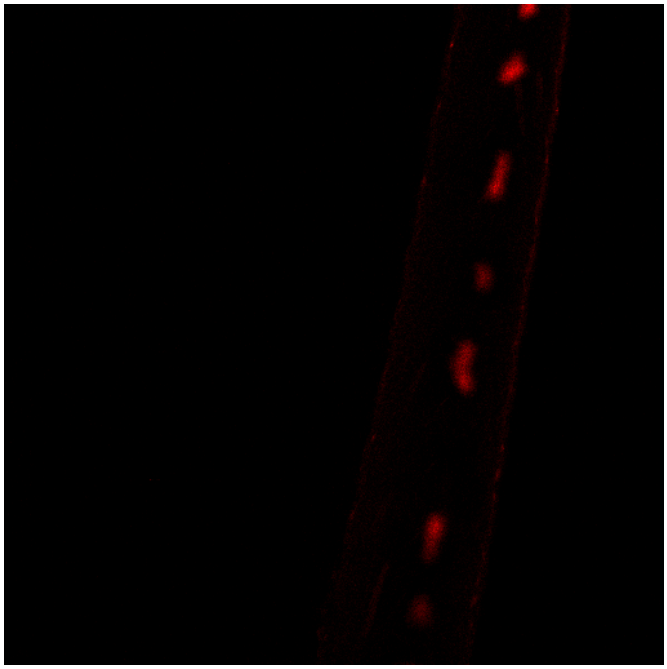

Figure 12. Confocal image of IR-LEGO exposed medaka with only visible natural flourescence

Spinning disk confocal microscopy is a form of confocal microscopy that prioritizes the safety of biological samples. It does this by rapidly spinning a disk with many

pinholes in it before exposure to the sample in order to reduce the time the laser is being exposed to the sample. This provides a much safer environment for the organisms, allowing for extended timelapse imaging to be taken as they are not a risk of being destroyed by the laser.

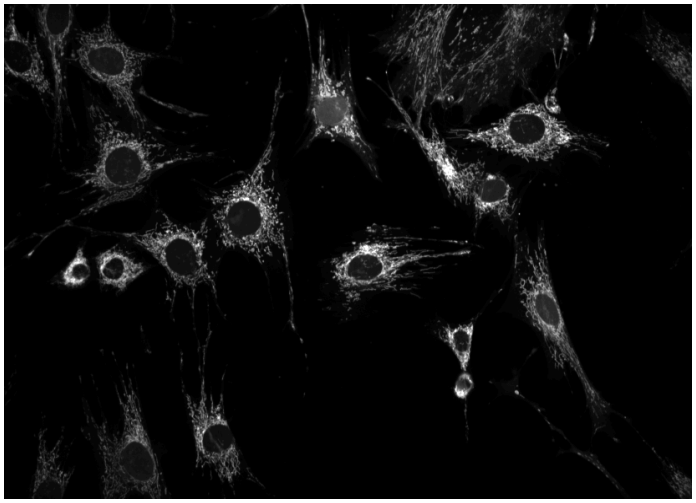

Figure. 13 Scanning disk image of samples we observed for 24 hrs.

Scanning electron microscopy uses electrons instead of light in order to scan a sample's surface and produce extremely high resolution images. This is mostly used to examine dimensional topography and distribution of exposed features (Fischer 2012). This method is not a quick and easy process, often time for the best images samples need to be coated with certain reagents, along with being destructive to most biological samples. I used this technology to take images of aphids and a pillbugv for a collaborator, but we did not coat our samples as it was a quick demonstration and not a publication-quality request.

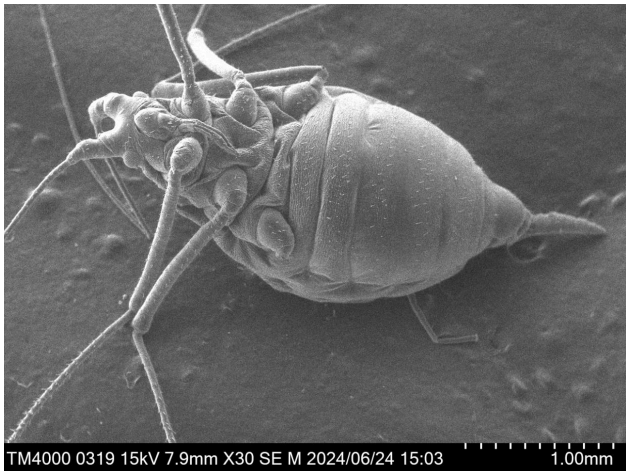

Figure 14. Pregnant aphid SEM photo

Phase Contrast Microscopy is used to enhance the contrast of transparent and colorless specimens without staining or altering. It is usually used to visualise cells and cell compotnents that would be difficult to see using an ordinary light microscope. It is versatile and very simple compared to fluorescent microscopy, not requiring any steps beforehand such as fluorescent markers or staining (Yin Z 2012) . It is ideal for thinner samples. A phase plate is used to intensify the extremely small differences in light phase caused by the specimen, and making it more apparent to the human eye.

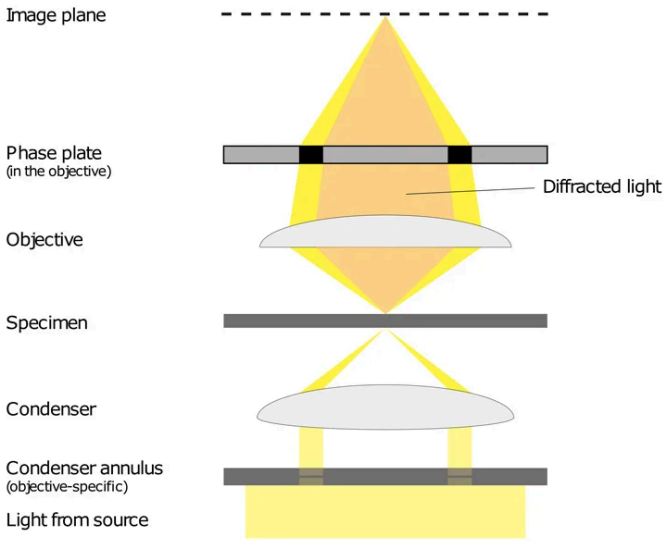

Figure 15. Path of light in a phase contrast microscope (A guide to phase contras, scientifica.uk.com)

I used this technology to take images of our muscle stem cells on the silanized glass.

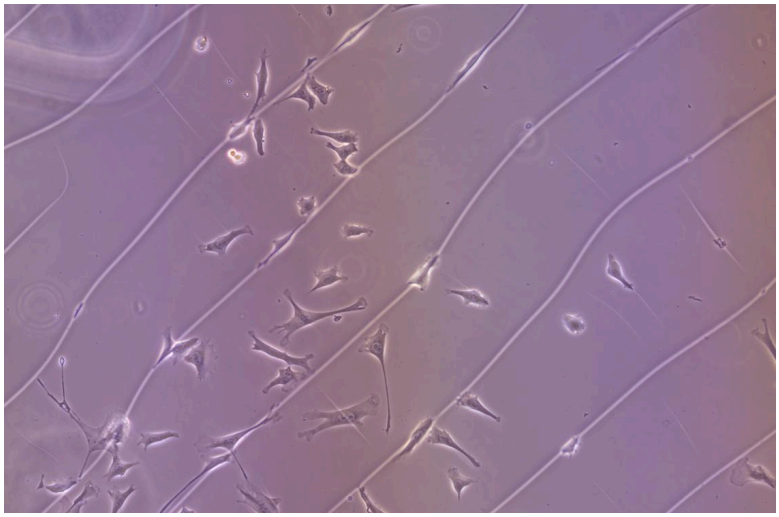

Figure 16. Silanized glass phase contrast image of muscle stem cells

Atomic Force Microscopy utilizes a photodiode to detect changes in laser position based on its reflection off of an extremely small cantilever. This type of microscopy is useful for generating images of extremely small objects such as individual molecules, or

for generating data on kPa resistance and elasticity of materials. In my applications of this technology we did not use it for imaging, but for generating data on gel rigidity and elasticity for the silanizing glass experiment.

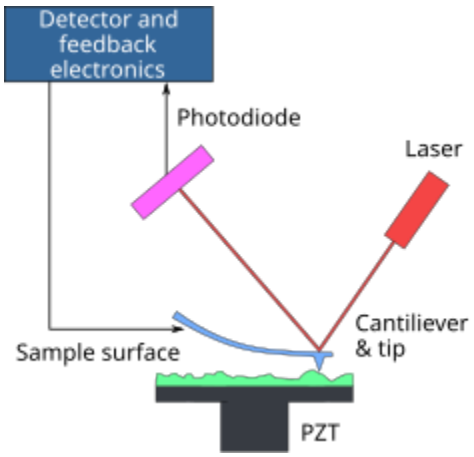

Figure 17. Construction of an atomic force microscope

Acknowledgment:
Thank you to the NSF for providing funding to this amazing opportunity and promoting international collaboration. Thank you to the Kamei lab for taking care of me by providing mentorship and guidance in a foreign country. Thank you to Dr. Munakata and Dr. Molina for hosting this experience and providing support as well.

Data index:

Gel spread data

UNLABELED	GLASS					
Pos 1	Area	Mean	Circ.	AR	Round	Solidity
1	740.816	110.886	0.14	8.479	0.118	0.492
2	911.374	108.567	0.12	4.379	0.228	0.393
3	593.31	113.422	0.435	1.765	0.567	0.748
4	540.459	119.425	0.461	2.469	0.405	0.753
5	457.27	117.599	0.352	2.275	0.44	0.657
6	520.692	129.632	0.626	2.408	0.415	0.884
7	762.733	111.227	0.15	3.506	0.285	0.481
8	1065.80	118.979	0.154	2.522	0.396	0.422
9	1273.15	118.192	0.391	2.074	0.482	0.67
Pos 2	Area	Mean	Circ.	AR	Round	Solidity
1	554.433	102.807	0.501	2.093	0.478	0.764
2	325.649	106.965	0.216	4.081	0.245	0.54
3	726.902	115.11	0.422	2.037	0.491	0.701
4	723.498	121.568	0.259	2.885	0.347	0.623
5	499.193	109.486	0.39	1.596	0.627	0.778
6	668.078	122.115	0.234	2.509	0.399	0.65
Pos 3	Area	Mean	Circ.	AR	Round	Solidity
1	827.529	109.064	0.243	3.053	0.328	0.48
2	1029.26	118.308	0.247	3.583	0.279	0.593
3	912.688	120.2	0.144	6.322	0.158	0.436
4	259.062	129.784	0.361	2.689	0.372	0.702
5	359.45	105.009	0.225	6.8	0.147	0.624
6	1061.50	118.28	0.219	3.816	0.262	0.614
7	545.654	112.52	0.116	3.062	0.327	0.331
8	451.477	100.97	0.124	2.159	0.463	0.346
9	1148.69	129.367	0.201	5.075	0.197	0.54
10	814.39	138.031	0.53	1.813	0.552	0.842
Pos 4	Area	Mean	Circ.	AR	Round	Solidity
1	710.598	132.144	0.241	2.173	0.46	0.573
2	371.931	130.679	0.112	3.548	0.282	0.323
3	779.455	131.862	0.154	1.556	0.643	0.395
4	787.457	120.652	0.124	2.369	0.422	0.278
5	257.748	147.212	0.328	2.054	0.487	0.652
6	348.282	146.906	0.223	7.103	0.141	0.64
7	2371.98	125.037	0.084	2.111	0.474	0.343
8	897.639	127.252	0.265	2.66	0.376	0.603
9	1838.63	121.719	0.187	3.137	0.319	0.48
10	201.552	159.641	0.291	3.375	0.296	0.652
Pos 5	Area	Mean	Circ.	AR	Round	Solidity
1	381.426	135.952	0.152	2.115	0.473	0.441
2	363.093	131.132	0.145	2.28	0.439	0.314
3	511.495	137.996	0.424	1.352	0.74	0.662
4	311.495	136.46	0.485	2.244	0.446	0.823
5	899.251	133.83	0.245	4.429	0.226	0.596
6	951.685	137.877	0.216	2.478	0.403	0.512
7	916.988	145.582	0.236	4.331	0.231	0.643
8	685.457	134.549	0.088	4.411	0.227	0.223
9	581.605	138.168	0.217	4.694	0.213	0.545
Pos 6	Area	Mean	Circ.	AR	Round	Solidity
1	882.59	126.387	0.247	5.993	0.167	0.683
2	768.825	120.443	0.116	1.826	0.547	0.308
3	2106.29	118.878	0.276	3.691	0.271	0.679
4	422.453	111.866	0.15	4.046	0.247	0.411
5	601.014	108.075	0.16	4.151	0.241	0.429
6	698.834	103.242	0.152	1.667	0.6	0.345
7	851.775	126.47	0.118	10.603	0.094	0.386
8	553.716	132.924	0.141	7.823	0.128	0.455
9	911.792	114.271	0.096	2.071	0.483	0.212
10	570.617	127.131	0.118	1.687	0.593	0.396
11	926.782	126.746	0.227	3.721	0.269	0.523
Stdev	Area		Stdev	AR		
410.4495	749.7373		1.899643	3.439072		

0.05	Gel						
Pos 1	Area	Mean	Min	Max	Circ.	AR	Round	Solidity
1	523.596	186.377	162	236	0.374	3.859	0.259	0.659
2	197.03	191.242	157	239	0.477	2.856	0.35	0.902
3	164.86	183.379	158	234	0.383	2.239	0.447	0.7
4	328.23	175.077	149	218	0.274	4.402	0.227	0.584
5	256.953	180.701	154	234	0.209	8.568	0.117	0.568
6	447.044	182.761	143	240	0.343	4.244	0.236	0.676
7	585.01	197.098	165	242	0.291	5.991	0.167	0.636
8	510.121	195.075	162	245	0.436	4.361	0.229	0.839
Pos 2	Area	Mean	Min	Max	Circ.	AR	Round	Solidity
1	437.697	228.336	208	254	0.27	6.57	0.152	0.651
2	554.389	229.647	209	249	0.192	10.005	0.1	0.756
3	699.18	199.685	182	228	0.192	2.04	0.49	0.38
4	492.631	202.357	164	241	0.174	7.523	0.133	0.491
Pos 3	Area	Mean	Min	Max	Circ.	AR	Round	Solidity
1	315.557	176.978	139	238	0.347	3.279	0.305	0.667
2	408.968	171.541	136	230	0.217	3.149	0.318	0.542
3	776.42	217.818	171	254	0.137	8.077	0.124	0.567
4	760.536	243.926	212	254	0.159	2.39	0.418	0.355
5	264.809	239.15	190	254	0.326	1.27	0.787	0.658
Pos 4	Area	Mean	Min	Max	Circ.	AR	Round	Solidity
1	395.378	158.222	119	225	0.193	7.111	0.141	0.559
2	628.992	161.622	123	209	0.317	1.647	0.607	0.566
3	188.715	183.449	139	255	0.427	3.745	0.267	0.77
4	406.445	173.273	129	242	0.317	3.626	0.276	0.59
5	329.663	171.22	128	233	0.327	3.375	0.296	0.735
6	569.47	185.485	135	255	0.194	4.703	0.213	0.46
7	307.127	227.765	193	254	0.108	11.685	0.086	0.446
8	404.897	238.945	211	255	0.205	8.417	0.119	0.751
9	763.805	169.801	134	238	0.26	6.426	0.156	0.632
Pos 5	Area	Mean	Min	Max	Circ.	AR	Round	Solidity
1	458.684	206.622	166	249	0.128	3.343	0.299	0.36
2	1026.09	206.138	154	255	0.303	3.498	0.286	0.641
3	744.71	206.232	168	254	0.279	3.476	0.288	0.542
4	693.388	209.261	171	251	0.229	7.408	0.135	0.587
5	383.049	220.32	190	253	0.617	2.172	0.46	0.88
6	1003.66	213.203	177	245	0.509	2.076	0.482	0.824
7	519.238	205.673	182	230	0.277	1.217	0.822	0.504
8	383.508	207.049	166	247	0.436	2.688	0.372	0.739
9	423.935	173.542	144	214	0.257	6.415	0.156	0.629
Pos 6	Area	Mean	Min	Max	Circ.	AR	Round	Solidity
1	662.71	166.33	130	208	0.189	1.647	0.607	0.384
2	446.757	172.205	137	229	0.382	3.138	0.319	0.698
3	309.421	157.889	131	231	0.138	5.938	0.168	0.511
4	590.572	167.207	139	210	0.276	3.96	0.253	0.644
5	208.326	158.327	135	188	0.595	1.947	0.514	0.859
6	417.455	159.572	131	204	0.388	1.596	0.627	0.711
7	353.46	159.688	124	197	0.354	4.434	0.226	0.68
Pos 7	Area	Mean	Min	Max	Circ.	AR	Round	Solidity
1	330.179	185.767	161	220	0.314	3.599	0.278	0.67
2	312.403	184.093	163	211	0.15	1.828	0.547	0.401
3	564.596	196.217	174	240	0.235	4.212	0.237	0.491
4	273.582	193.182	163	241	0.06	7.333	0.136	0.244
5	317.22	198.99	174	238	0.252	2.973	0.336	0.526
6	192.499	196.346	171	234	0.502	2.122	0.471	0.756
7	215.723	193.781	175	234	0.296	3.05	0.328	0.62
8	209.53	200.227	174	244	0.269	2.339	0.428	0.553
9	185.676	206.094	180	245	0.324	1.312	0.762	0.572
10	342.221	213.729	187	245	0.4	2.551	0.392	0.702
11	351.797	217.931	192	250	0.447	3.554	0.281	0.779
12	337.462	220.368	192	254	0.189	8.072	0.124	0.616
13	386.719	213.362	182	243	0.36	3.425	0.292	0.624
Stdev	Area		Stdev	AR				
197.4063	442.9473		2.412198	4.2342				

0.2		Gel						
Pos 1	Area	Mean	Min	Max	Circ.	AR	Round	Solidity
1	438.844	143.329	108	203	0.1	5.01	0.2	0.333
2	1060.38	150.763	115	211	0.313	1.242	0.805	0.672
3	272.263	168.094	117	242	0.282	5.062	0.198	0.707
4	756.293	149.483	118	226	0.205	5.662	0.177	0.533
5	548.368	154.291	122	226	0.19	6.779	0.148	0.49
6	652.503	166.318	122	243	0.335	2.598	0.385	0.698
7	595.905	159.297	125	234	0.399	3.058	0.327	0.771
8	394.231	162.814	126	219	0.603	1.329	0.752	0.818
9	350.077	160.14	116	233	0.163	14.318	0.07	0.636
Pos 2	Area	Mean	Min	Max	Circ.	AR	Round	Solidity
1	646.31	168.535	119	230	0.332	5.624	0.178	0.769
2	1391.19	155.609	120	203	0.443	1.982	0.505	0.781
3	1717.07	152.35	122	183	0.437	1.607	0.622	0.695
4	609.782	149.85	114	228	0.445	1.404	0.712	0.696
5	918.286	147.76	116	174	0.448	3.216	0.311	0.844
6	565.514	150.622	117	202	0.182	3.654	0.274	0.411
7	930.844	151.594	119	197	0.408	1.904	0.525	0.742
8	255.519	148.673	122	213	0.25	4.941	0.202	0.655
9	569.356	157.519	116	212	0.131	12.003	0.083	0.526
10	781.925	159.029	119	209	0.192	7.251	0.138	0.531
11	626.813	159.706	125	208	0.174	6.681	0.15	0.492
12	520.729	155.163	124	199	0.141	2.933	0.341	0.363
Pos 3	Area	Mean	Min	Max	Circ.	AR	Round	Solidity
1	503.698	162.369	135	224	0.176	5.567	0.18	0.478
2	813.922	156.175	134	189	0.303	2.628	0.381	0.628
3	550.203	154.653	132	191	0.166	3.378	0.296	0.5
4	950.455	158.66	132	212	0.132	8.184	0.122	0.417
5	369.803	156.616	131	204	0.242	1.738	0.575	0.503
6	268.995	163.863	134	219	0.309	2.903	0.344	0.629
7	423.476	152.689	132	191	0.145	1.551	0.645	0.305
8	528.47	156.352	132	197	0.312	4.433	0.226	0.625
9	323.355	155.635	130	209	0.219	5.912	0.169	0.665
10	299.386	166.454	140	227	0.306	6.566	0.152	0.859
11	628.82	164.026	138	220	0.246	4.76	0.21	0.535
12	359.252	171.438	142	227	0.404	3.37	0.297	0.815
13	223.579	177.753	142	237	0.39	2.74	0.365	0.668
14	788.347	161.342	132	212	0.154	2.551	0.392	0.393
15	408.051	161.023	137	255	0.148	1.408	0.71	0.302
16	369.574	162.649	134	220	0.175	4.965	0.201	0.504
Pos 4	Area	Mean	Min	Max	Circ.	AR	Round	Solidity
1	429.956	159.913	127	234	0.338	3.734	0.268	0.68
2	618.728	151.866	120	221	0.174	3.868	0.258	0.476
3	397.672	153.45	125	216	0.235	5.914	0.169	0.557
4	838.809	150.035	120	199	0.163	5.534	0.181	0.438
5	588.451	145.847	120	208	0.164	6.305	0.159	0.467
6	548.368	148.997	129	177	0.233	1.412	0.708	0.547
7	556.912	149.689	120	202	0.347	2.531	0.395	0.688
8	196.513	157.976	124	219	0.213	7.135	0.14	0.768
9	692.987	151.487	124	199	0.379	2.574	0.388	0.698
10	289.695	160.032	134	227	0.392	3.61	0.277	0.734
11	502.494	167.867	129	231	0.516	2.618	0.382	0.839
12	752.623	157.593	131	205	0.197	3.508	0.285	0.519
13	436.665	161.422	132	214	0.428	2.454	0.407	0.688
14	495.67	149.979	124	192	0.106	3.64	0.275	0.357
Pos 5	Area	Mean	Min	Max	Circ.	AR	Round	Solidity
1	360.055	206.816	172	241	0.141	1.687	0.593	0.282
2	206.319	209.457	173	249	0.115	13.638	0.073	0.43
3	150.582	222.549	180	255	0.402	1.58	0.633	0.687
4	395.607	219.275	186	252	0.33	5.919	0.169	0.668
5	481.335	197.216	169	233	0.233	1.654	0.605	0.494
6	321.807	209.513	178	246	0.323	4.511	0.222	0.742
7	240.839	203.923	174	244	0.156	1.695	0.59	0.332
8	783.76	199.58	174	232	0.113	6.725	0.149	0.512
9	619.244	213.253	182	250	0.172	11.886	0.084	0.636
Stdev	Area		Stdev	AR				
278.7054	555.2780		2.935657	4.4174				

References:

A guide to phase contrast: Principles, applications and setup. A Guide to Phase Contrast | Principles, Applications and Setup. (n.d.). https://www.scientifica.uk.com/learning-zone/a-guide-to-phase-contrast#:~:text=Phase%20Contrast%20is%20a%20light,using%20an%20ordinary%20light%20microscope.

B.-C. Chen, W. R. Legant, K. Wang, L. Shao, D.E. Milkie, M.W. Davidson, C. Janetopoulos, X.S. Wu, J.A. Hammer, Z. Liu, B.P. English, Y. Mimori-Kiyosue, D.P. Romero, A.T. Ritter, J. Lippincott-Schwartz, L. Fritz-Laylin, R.D. Mullins, D.M. Mitchell, J.N. Bembenek, A.C. Reymann, R. Böhme, S.W. Grill, J.T. Wang, G. Seydoux, U.S. Tulu, D.P. Kiehart, E. Betzig (2014) *Lattice light-sheet microscopy: Imaging molecules to embryos at high spatiotemporal resolution,* Science 346, 1257998.

Elliott AD. Confocal Microscopy: Principles and Modern Practices. Curr Protoc Cytom. 2020 Mar;92(1):e68. doi: 10.1002/cpcy.68. PMID: 31876974; PMCID: PMC6961134.
Kamei, Y., Suzuki, M., Watanabe, K., Fujimori, K., Kawasaki, T., Deguchi, T., Yoneda, Y., Todo, T., Takagi, S., Funatsu, T., and Yuba, S. (2009). Infrared laser-mediated gene induction in targeted single cells *in vivo*. Nat. Methods *6*, 79-81.

Fischer ER, Hansen BT, Nair V, Hoyt FH, Dorward DW. Scanning electron microscopy. Curr Protoc Microbiol. 2012 May;Chapter 2:Unit 2B.2.. doi: 10.1002/9780471729259.mc02b02s25. PMID: 22549162; PMCID: PMC3352184.

Gull, M. (Ed.). (2019). Plasmid. IntechOpen. doi: 10.5772/intechopen.71424

Hayashi K, Matsuda M, Nakahata M, Takashima Y, Tanaka M. Stimulus-Responsive, Gelatin-Containing Supramolecular Nanofibers as Switchable 3D Microenvironments for Cells. Polymers (Basel). 2022 Oct 19;14(20):4407. doi: 10.3390/polym14204407. PMID: 36297985; PMCID: PMC9607093.

Lu, K., Wazawa, T., Sakamoto, J., Quang, C., Nakano, M., Kamei, Y., Nagai, T. (2022). Intracellular Heat Transfer and Thermal Property Revealed by Kilohertz Temperature Imaging with a Genetically Encoded Nanothermometer. Nano Letters *22*, 5698-5707.

Minuti AE, Labusca L, Herea DD, Stoian G, Chiriac H, Lupu N. A Simple Protocol for Sample Preparation for Scanning Electron Microscopic Imaging Allows Quick Screening of Nanomaterials Adhering to Cell Surface. Int J Mol Sci. 2022 Dec 27;24(1):430. doi: 10.3390/ijms24010430. PMID: 36613905; PMCID: PMC9820490.

Shimada, A., Kawasishi, T., Kaneko, T., Yoshihara, H., Yano, T., Inohaya, K., Kinoshita, M., Kamei, Y., Tamura, K. and Takeda, H. (2013). Trunk exoskeleton in teleosts is mesodermal in origin. Nat. Commun. *4*, 1639.
Stelzer, E.H.K., Strobl, F., Chang, BJ. *et al.* Light sheet fluorescence microscopy. *Nat Rev Methods Primers* 1, 73 (2021). https://doi.org/10.1038/s43586-021-00069-4

Yin Z, Kanade T, Chen M. Understanding the phase contrast optics to restore artifact-free microscopy images for segmentation. Med Image Anal. 2012 Jul;16(5):1047-62. doi: 10.1016/j.media.2011.12.006. Epub 2012 Feb 3. PMID: 22386070; PMCID: PMC3372640.